Institut für Geowissenschaften Jena

Transdimensional Bayesian approach to seismic traveltime tomography applied on field data from the Salzach Valley.

Francesco Fontanini and *Florian Bleibinhaus*

Friedrich-Schiller-Universität Jena

seit 1558

1. INTRODUCTION

A meaningful interpretation of seismic measurements requires a rigorous quantification of the uncertainty. We are developing a technique that allows a quantitative estimation of the uncertainty in seismic traveltime tomography. A bayesian algorithm has been included in the existing simulr16(1) code in order to allow the inversion of reflection-refraction data also with a probabilistic approach, obtaining as a solution an ensemble of models. The probability distribution for the inverse parameters in this ensemble contains much more informations than a single deterministic solution model and allows a quantitative assessment of model parameters uncertainty.

(1) simulr16: Thurber CH (1983) - Bleibinhaus F and Gebrande H (2006) - Bleibinhaus F and Hilberg (2012) - Vidale JE (1990)

2. MCMC ALGORITHM SCHEME

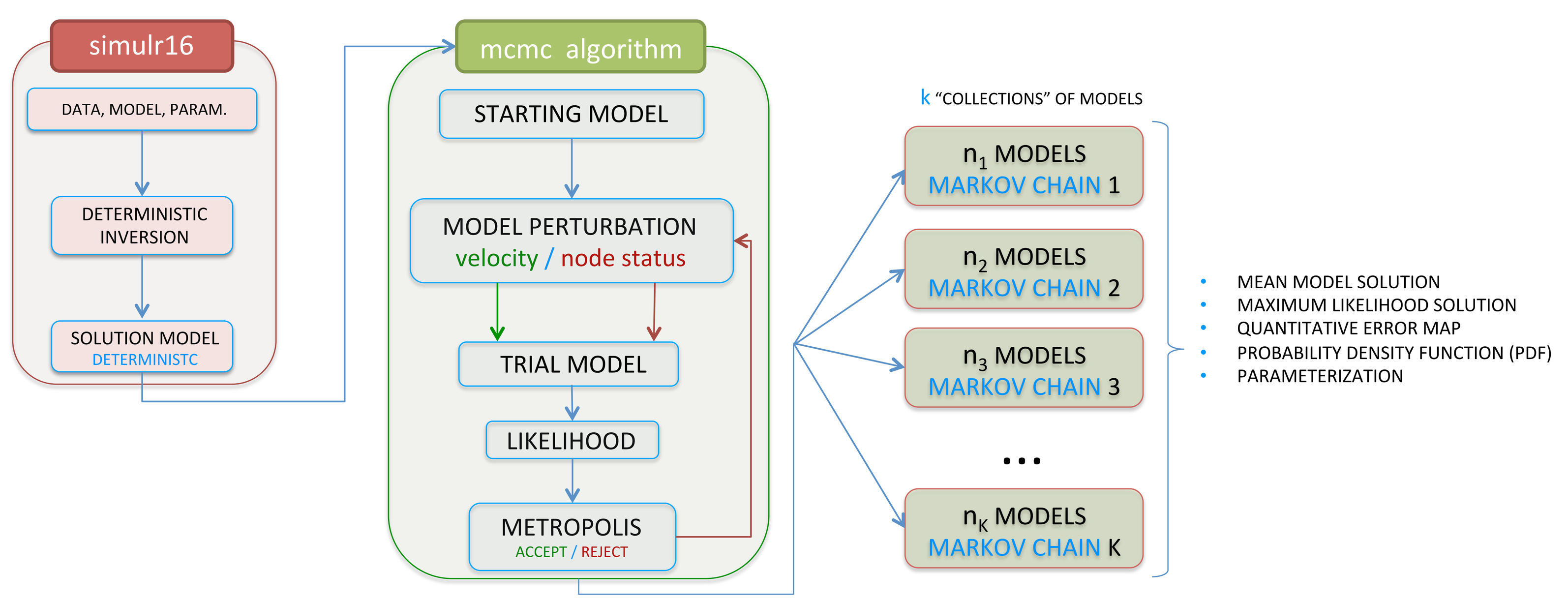

3. TEST SYNTHETIC MODEL

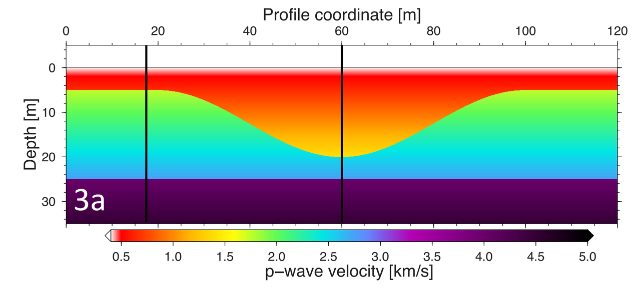

FIG.3a
synthetic model: 23 sources, 23 receivers, spacing 5 m. The travel times are computed with an external eikonal solver(2) then inverted with the transdimentional *simul* code.

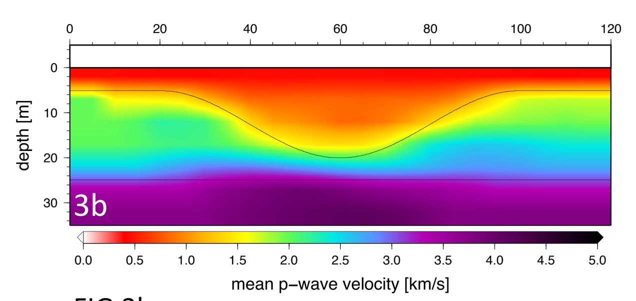

FIG.3b
mean model: obtained computing the average value of the velocity for each node position over the population of accepted models.

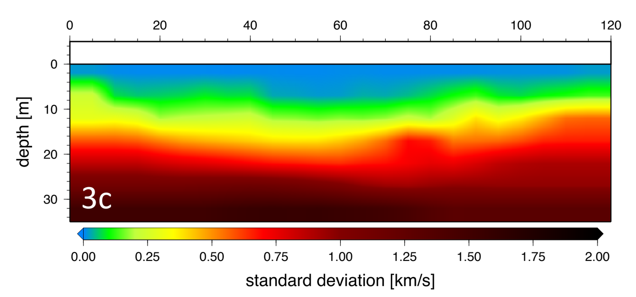

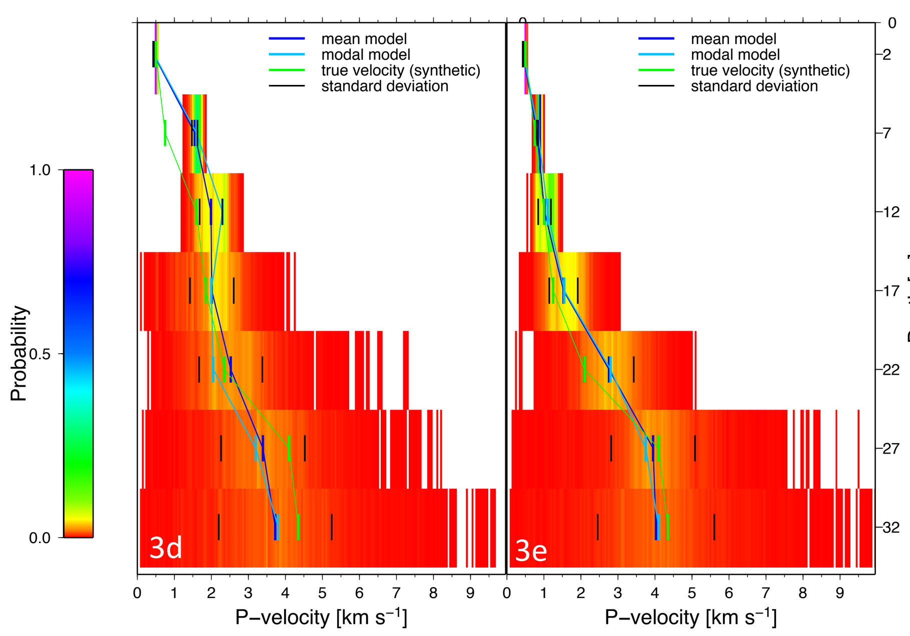

FIG.3d-e
probability density function: the "solution" of a bayesian inversion is the probability density function (PDF), that in this case can be regarded as the probability to have a certain velocity value for each given depth. Here the PDF is plotted for 7 depths and 2 profile positions (black vertical lines in FiG.3a) corresponding to 17m (FIG. 3d) and 60m (FIG.3e).

The **aim** of a probabilistic inversion is not to provide an optimal solution, but to provide a global overview on the probability distribution of the inverted parameters; all the possible values for a parameter are displayed along with their probability.

FIG.3c
error map: the standard deviation can be computed for every node in the model providing a quantitative estimation of the uncertainty of a possible solution.

(2) J. A. Hole and B. C. Zelt *Geophys. J. Int.* (1995) **121**, 427–434 ; 3-D finite difference reflection traveltimes

CONTACTS:

francesco.fontanini@uni-jena.de,
florian.bleibinhaus@uni-jena.de
Friedich Schiller Universität Jena,
Institut für Geowissenschaften
Burgweg 11 - 07749 - Jena - DE

FWF Der Wissenschaftsfonds.

4. SALZACH VALLEY SURVEY(3)

- SALZACH VALLEY, AUSTRIA (FIG.4a)
- 3 Km WIDE-ANGLE-SEISMIC SURVEY (FIG.4b)
- 10 Hz GEOPHONES, 10 m SPACING
- 8 EXPLOSIVE SOURCES (SP)
- REFLECTION AND REFRACTION TRAVELTIME TOMOGRAPHY

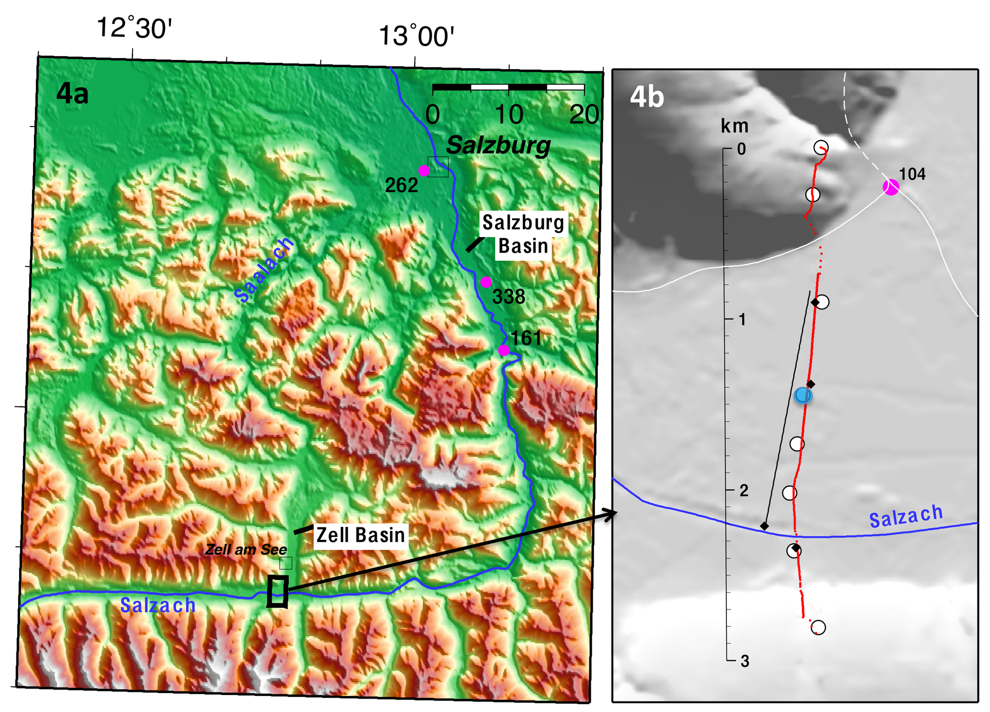

(3) Florian Bleibinhaus and Sylke Hilberg. *Geophys. J. Int.* (2012) **189**, 1701–1716
Shape and structure of the Salzach Valley, Austria, from seismic traveltime tomography and full waveform inversion

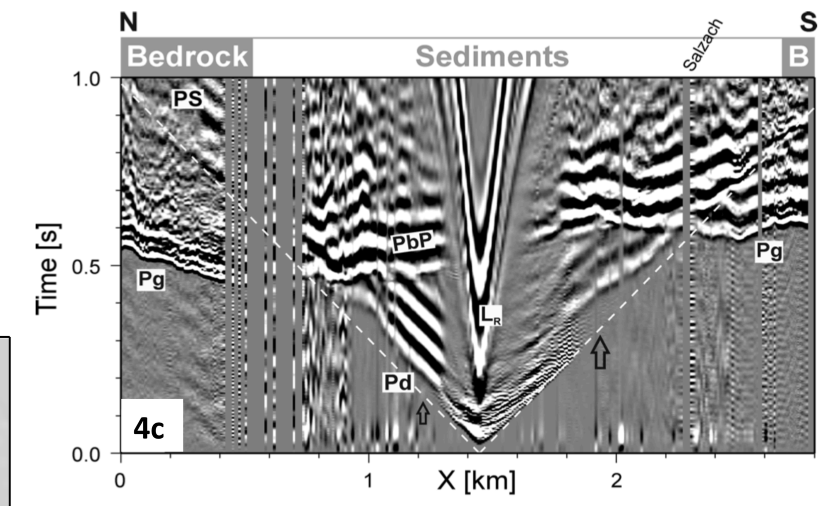

FIG.4c SP 4 (blue dot in fig.4b) in the centre of the valley. The arrows denote shadow zones. White dashed line is 1500 m s–1. (b) SP 8 on bedrock. Pd, direct wave; Pg, bedrock refraction; PbP, bedrock reflection; LR, Rayleigh waves; PS, *P*-wave converted to *S* at the sediment-bedrock contact.

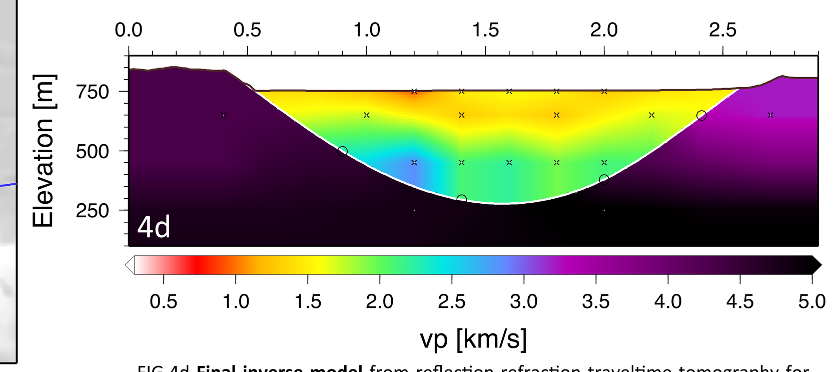

FIG.4d **Final inverse model** from reflection-refraction traveltime tomography for an adjusted, irregular grid.

5. TRANSDIMENSIONAL BAYESIAN MCMC INVERSION

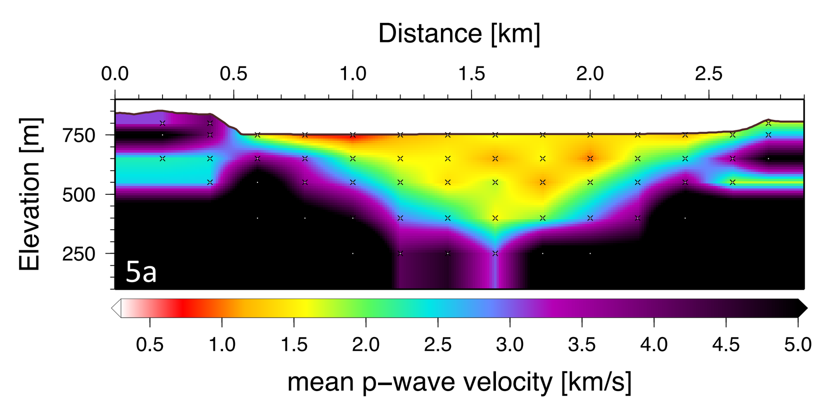

FIG.5a
mean model: computed from an ensemble of 66384 models produced by our MCMC transdimensional algorithm.

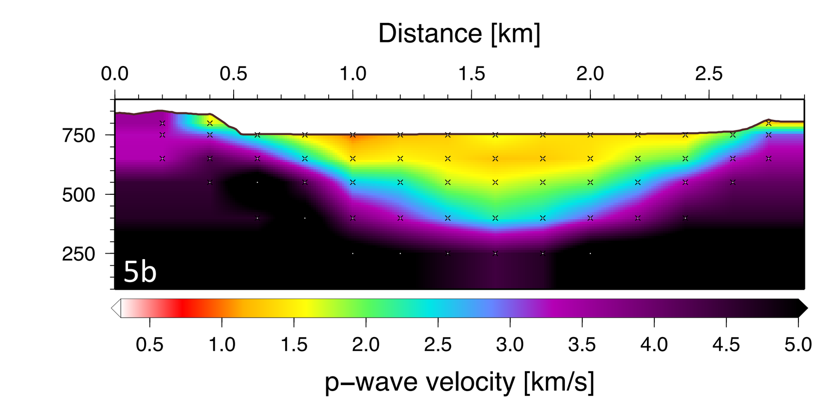

FIG.5b
deterministic solution: model from a deterministic inversion of refraction data only.

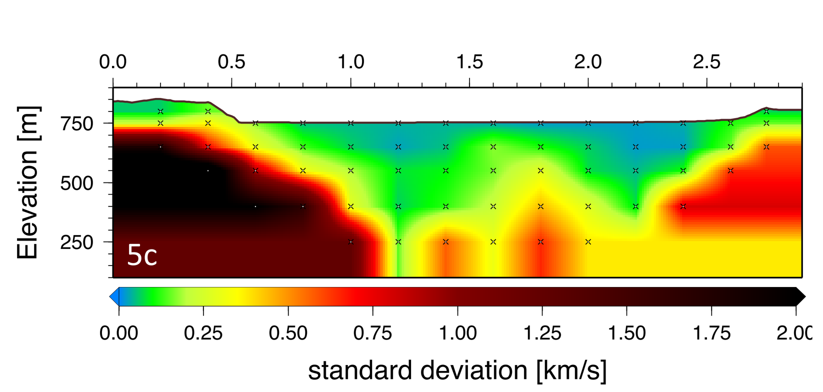

FIG.5c
error map: the standard deviation can be computed for every node in the model providing in this way a quantitative estimation of the uncertainty of a possible solution.

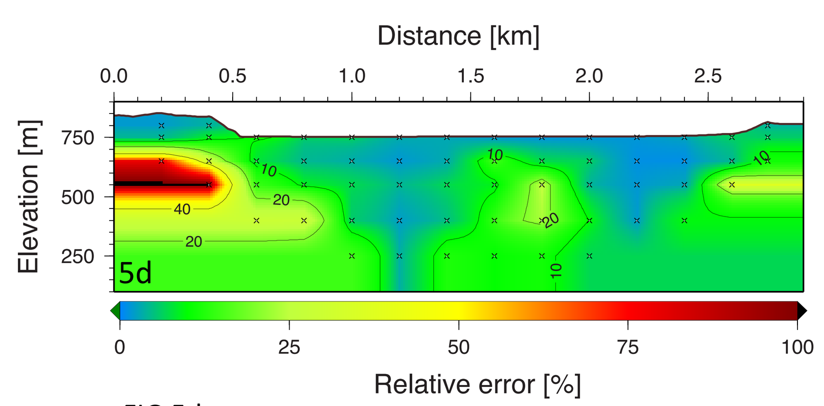

FIG.5d
relative error map: the percentage error gives a more direct visualization of the areas of the model affected by an higher uncertainty.

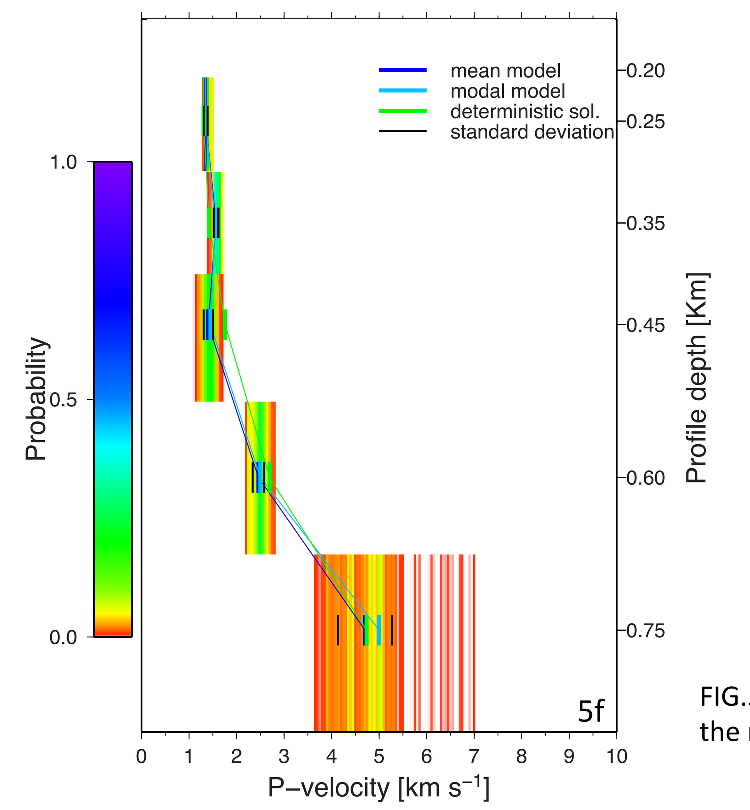

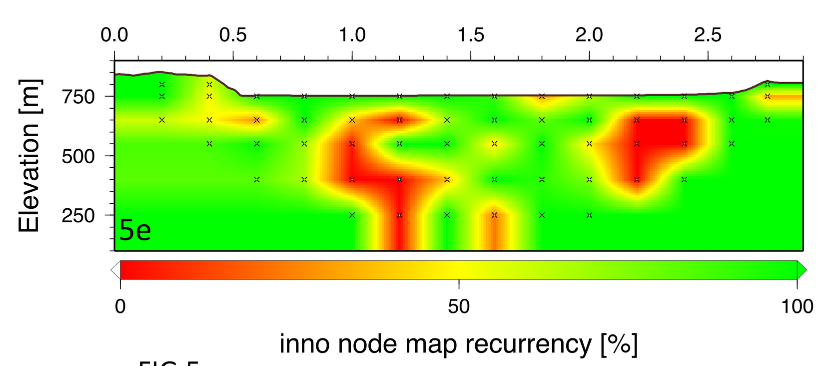

FIG.5e
node recurrency: displays how frequently a node has been used as an inversion parameter. This map could be an additional tool to estimate well constrained nodes and evaluate and optimal parameterization.

FIG.5f **PDF:** posterior probability distribution for six parameters corresponding to the nodes located at profile position 1.4 Km

6. IMPROVING THE EFFICIENCY: MULTIPLE MARKOV CHAINS

A major issue connected with MCMC methods is the computation time required to sample enough models to saturate the PDF, hence to obtain stationary solution maps that well represent the posterior mean and variance. An easy way to increase the speed of the sampling process is to run multiple instances of an MCMC algorithm, producing multiple Markov Chains and then merging them. The speedup obtained is in this way directly proportional to the number of processes that are run on independent cores/CPUs. The average solution from multiple chains is, moreover, less affected by local minima since the model space will be sampled with independent processes that are not likely to be all trapped in the same local minimum.

SINGLE CHAIN*		20 CHAINS
1.015.312	MCMC ITERATIONS	20.306.248
14d, 3h	COMPUTATION TIME	14d, 3h
66.384	MODELS ACCEPTED	1.327.682
20	SAVING INTERVAL	20
3319	MODELS SAVED	66375
6,52 %	ACCEPTANCE RATE	6,54 %
20,16 sec	TIME/MODEL	0.90 sec

*average on 20 chains

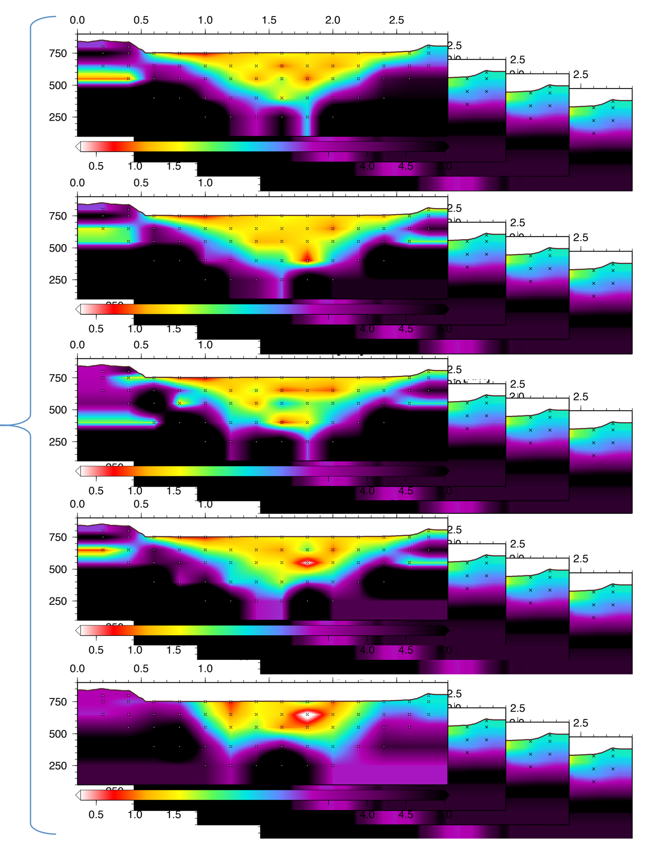

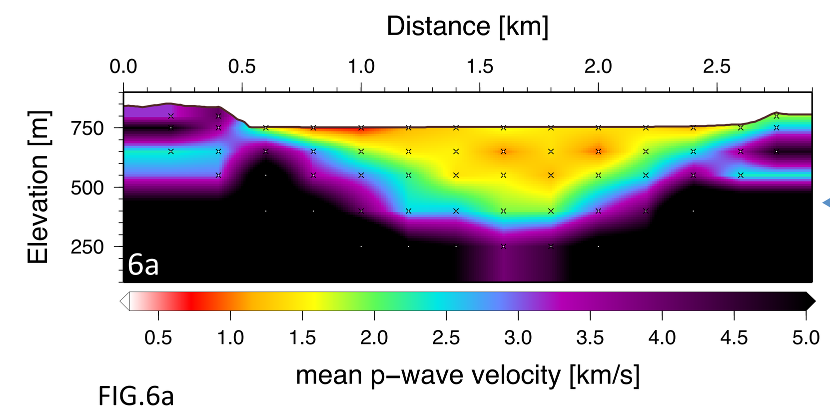

FIG.6a
multiple chains mean model: all the models sampled from the 20 markov are merged into a single ensemble of models. 66000 models have been used in the computation of this average.

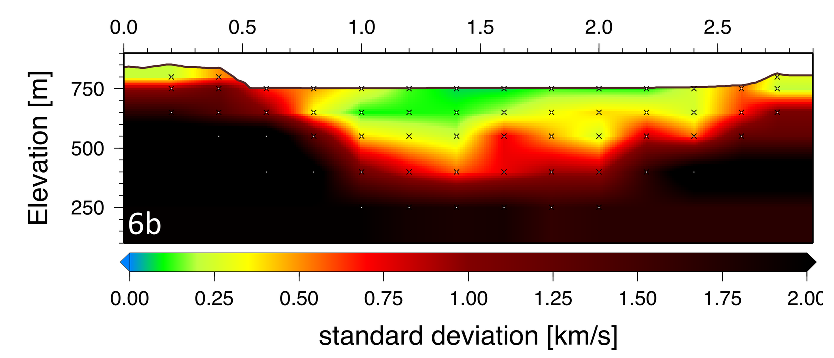

FIG.6b
multiple chains error maps: obtained averaging the single error maps.

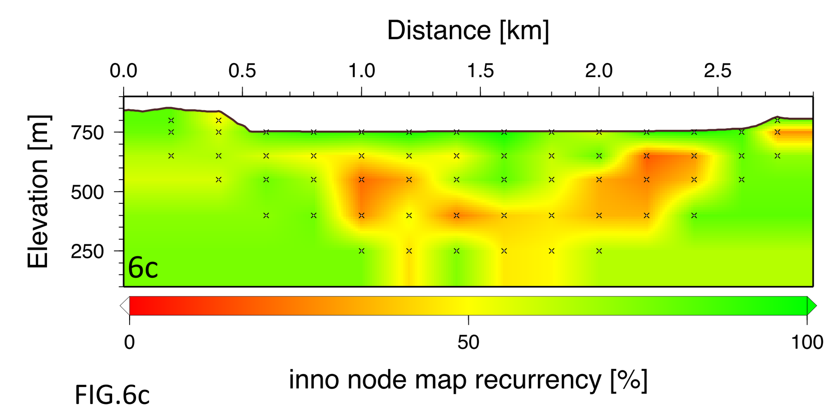

FIG.6c
node map: averaging the node maps from the single inversions results in a smoother map hence in a more uniform sampling of the model space.

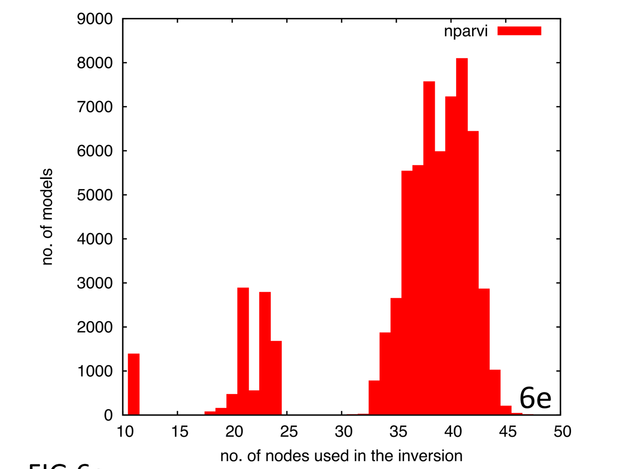

FIG.6e
number of parameters: posterior distributions on the number of inverse parameters for the ensemble obtained merging the 20 Markov Chains. The multimodal distribution suggests that some of the chains sampled areas of the model space corresponding to some local minima.

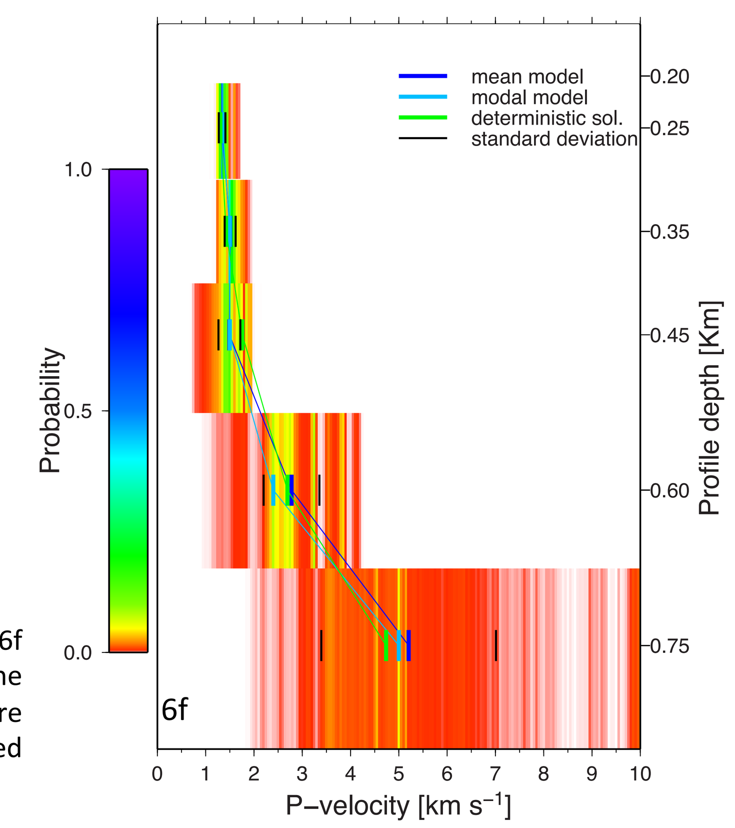

FIG.6f
multiple chains PDF: obtained from the models sampled by the 20 independent chains. The model space has been sampled more exhaustively, the saturation of the PDF can be therefore reached in a shorter time.

7. FUTURE DIRECTIONS

In order to increase the acceptance ratio of sampled models, we are implementing the use of the off-diagonal elements of the resolution matrix to obtain a set of trade-off relations between different inverse parameters. Having a quantitative value to describe the inter-correlation between parameters will compensate global biasing effects of a random perturbation, allowing also to increase the magnitude of perturbations, finally resulting in a more efficient and fast sampling of the prior model space.